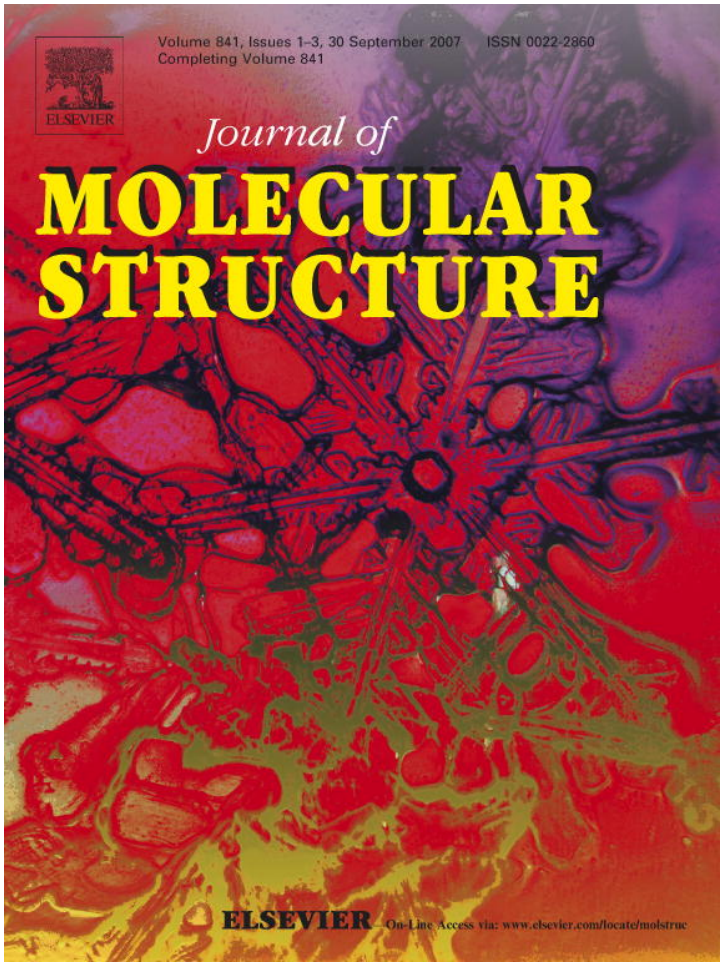

Available online at www.sciencedirect.com
ScienceDirect
Journal of Molecular Structure 841 (2007) 96–103
Journal of MOLECULAR STRUCTURE
www.elsevier.com/locate/molstruc

Synthesis and spectroscopic ^{27}Al NMR and Raman characterization of new materials based on the assembly of $[AlO_4Al_{12}(OH)_{24}(H_2O)_{12}]^{7+}$ isopolycation and Co–Cr and $[AlMo_6O_{24}H_6]^{3-}$ Anderson heteropolyanions

Mercedes Muñoz [a], Carmen I. Cabello [a,*], Irma L. Botto [b], Giuliano Minelli [c], Mickael Capron [d], Carole Lamonier [d], Edmond Payen [d]

[a] "Centro de Investigación y Desarrollo en Ciencias Aplicadas, Dr. J. J. Ronco", CINDECA-CONICET-Universidad Nacional de la Plata, 1900 La Plata, Buenos Aires, Argentina
[b] "Centro de Química Inorgánica" CEQUINOR-CONICET-Universidad Nacional de La Plata, 1900 La Plata, Buenos Aires, Argentina
[c] "Istituto di Sistemi Complessi", ISC – CNR, Dipartimento di Chimica, Università di Roma "La Sapienza", Piazzale Aldo Moro 5, Roma 00185, Italy
[d] "Unité de Catalyse et de chimie du solide", UCCS, UMR-CNRS 8181, Université des Sciences et Technologie de Lille, 59655 Villeneuve d'Ascq, Cedex, France

Received 5 July 2006; received in revised form 20 November 2006; accepted 27 November 2006
Available online 19 January 2007

Abstract

New advanced inorganic composite materials were prepared by combination of the polycation $[AlO_4Al_{12}(OH)_{24}(H_2O)_{12}]^{7+}$ with heteropolyoxomolybdates of Anderson type structure with formula: $[XMo_6O_{24}H_6]^{3-}$ where X = Al(III), Co(III), and Cr(III). The synthesis of these materials is performed by direct mixture of the isopolycation and heteropolyanions in a pH controlled aqueous solution. These new materials were characterized by X-ray powder diffraction (XRD), ^{27}Al nuclear magnetic resonance (NMR); vibrational (FT-IR and Raman Microprobe) and UV–visible diffuse reflectance (UV–vis-DR) spectroscopies and their stability was studied by thermal analysis (TG-DTA). The NMR and Raman spectroscopies are useful to characterize these materials and to demonstrate that the Anderson structure in the composite lattice is preserved. Likewise, XRD, Raman microprobe and UV–vis-DR spectroscopic techniques achieve the further characterization of thermal residues or intermediates. All results allow us to suggest that the evolution of properties depends on the heteroatom nature in the Anderson structural units of these new materials.

Keywords: Inorganic composites; Heteropolyanions; Al_{13}-isopolycation; ^{27}Al MAS NMR; Raman microprobe; Oxidative desulfurization; Hydrotreatment catalysts

1. Introduction

A new type of inorganic composite with the structural formula $[AlO_4Al_{13}(OH)_{24}(H_2O)_{12}][AlMo_6O_{24}H_6]_2\cdot(OH)\cdot 29.5H_2O$ (named Al_{13}–$AlMo_6$) has been recently reported by Ho Son et al. [1–3]. This composite was obtained through precipitation by mixing ammonium heptamolybdate [AHM] and $[AlO_4Al_{12}(OH)_{24}(H_2O)_{12}]^{7+}[Al_{13}]$ isopolycation chloride aqueous solutions. The structural characterization reveals the presence of the hexamolybdoaluminate (III) anion $[AlMo_6O_{24}H_6]^{3-}(AlMo_6)$ of Anderson structure orderly dispersed in a continuous matrix of $[Al_{13}]$ Keggin-arrangement.

It is well known that $[AlO_4Al_{12}(OH)_{24}(H_2O)_{12}]^{7+}$ Keggin type isopolycation $[Al_{13}]$ is a species widely used to pillar clays [4], process that leads to thermally stable materials of large application in catalysis. Likewise, the study of Anderson heteropolyanions (named XMo_6, where

* Corresponding author. Tel./fax: +54 221 4220288/4210711.
E-mail address: ccabello@quimica.unlp.edu.ar (C.I. Cabello).

0022-2860/$ - see front matter © 2006 Elsevier B.V. All rights reserved.
doi:10.1016/j.molstruc.2006.11.067

X = Al, Cr, Co) supported on alumina is part of a general project developed in our laboratory for the last ten years and directed to the preparation of hydrodesulfurization (HDS) and oxidative desulfurization (ODS) catalysts [5–9]. In fact, the formation of $AlMo_6$ entities has been evidenced during preparation of the oxidic precursor of these HDS catalysts [5]. These Anderson heteropolyanions (HPA) are versatile compounds that present a planar structure and permit to match different metallic elements as central heteroatoms, assuring a support uniformity in their deposition and offering redox and acid properties according to the nature of heteroatoms [8–10]. Recently, we have shown that the direct deposition of molybdocobaltate Anderson phase on alumina improves the performance of the $CoMo/Al_2O_3$ catalytic system widely applied in the industry for HDS process. Hence, this paper conducts to the direct preparation of Mo and CoMo based HDS oxidic precursor through a new arrangement route of Al_{13}–XMo_6 (X = Al, Co, Cr). The method is based on the direct combination of Al-isopolycation with different Anderson HPA in aqueous solution. Structural and spectroscopic characterizations of the three new phases were investigated by X-ray powder diffraction (XRD), vibrational FT-IR and Raman microprobe, solid state NMR and UV–visible diffuse reflectance (UV–vis-DR) spectroscopies, whereas their thermal stabilities were analyzed by thermogravimetric and differential thermal analysis (TG-DTA).

2. Experimental

2.1. Synthesis

The Al_{13} Keggin polycation solution was prepared according to the literature method [1,2]. A 2.5 M NaOH solution was added dropwise to a $0.3MAlCl_3{\cdot}6H_2O$ solution maintained between 80 and 90 °C for 1 h by refluxing under stirring. The hydrolysis ratio was $[OH^-/Al^{3+}] = 2.5$. The solution pH was 4.25 after cooling at room temperature.

Anderson ammonium salts $(NH_4)_3[XMo_6O_{24}H_6]{\cdot}7H_2O$ (hereafter named $CoMo_6$, $AlMo_6$ and $CrMo_6$) were obtained according to literature data by precipitation from aqueous solution of ammonium heptamolybdate (AHM), cobalt nitrate, and hydrogen peroxide for the former species [6–10]. AHM and aluminum or chromium nitrate were used for the synthesis of Al and Cr phases, respectively.

Composites of general formula $[AlO_4Al_{12}(OH)_{24}(H_2O)_{12}][XMo_6O_{24}H_6]_2(OH){\cdot}nH_2O$ (X = Al, Co, Cr) were prepared at room temperature by mixing the Al_{13} polycation solution with the corresponding Anderson heteropolyanion solution in the ratio $[Al/Mo + X] = 1.25$. Precipitation reaction occurred immediately upon mixing solutions. The precipitates were filtered off, washed with water and dried in air. For comparative purposes and to analyze the effectiveness of the proposed method, the Al_{13}–$AlMo_6$ phase was also prepared by combination of the polycation and AHM according to the recently above mentioned method [1]. The preparation was checked by XRD before its use as reference. The chemical analysis was performed by atomic absorption spectroscopy (AAS) with a spectrometer IL-457 after acid dissolution of the composite material.

2.2. Characterization

2.2.1. X-ray diffraction

Powder diffraction patterns were obtained with a Philips PW 1714 diffractometer using CuKα radiation and Ni filter (range 2θ between 5° and 70°).

2.2.2. Vibrational spectroscopy

FT-IR spectra were obtained by using the KBr pellet technique with a Bruker IFS 66 FT-IR equipment (range 400–4000 cm^{-1}). Raman spectra were recorded at room temperature with a Raman microprobe (Infinity from Jobin-Yvon) equipped with a photodiode array detector. The exciting light source was the 532 nm line of an Nd YAG laser and the resolution of spectra was 2 cm^{-1}.

2.2.3. UV–visible diffuse reflectance spectroscopy

UV–vis-DR spectra were registered in the 200–800 nm spectral range with a Varian Super Scan 3 double beam spectrophotometer equipped with a chamber of diffuse reflectance with an integrating sphere. Two types of internal standards were used, i.e., $BaSO_4$ and Al_{13}–$AlMo_6$, the latter was employed to analyze the charge transfer (CT) bands of Cr and Co heteroatoms.

2.2.4. NMR spectroscopy

^{27}Al magic angle spinning (MAS) NMR experiments were carried out on Bruker ASX400 (9.4 T) spectrometers operating at ^{27}Al Larmor frequencies 104.3 MHz using 4 mm MAS probehead. ^{27}Al MAS NMR spectra were recorded by using a single pulse acquisition with small pulse angle ($\pi/12$) to assure a quantitative excitation of the central transition [12] and recycle delay of 5 s. ^{27}Al NMR spectra were referenced at 0 ppm relative to a 1 M $Al(NO_3)_3$ aqueous solution (pH ~1).

2.2.5. SEM-EDAX analysis

Samples were also analyzed by Scanning Electron Microscopy with a Philips 505 microscope equipped with an EDAX 9100 analyzer useful to carry out a semi-quantitative chemical analysis. The technique was used to control the sample homogeneity and to verify the chemical composition after the different treatments.

2.2.6. TG/DTA thermal analysis

TG-DTA measurements were carried out in a Shimadzu Thermoanalyzer equipment, in air atmosphere, between room temperature and 800 °C. Heated samples at intermediate temperature were characterized by XRD and Raman spectroscopy.

3. Results and discussion

3.1. Chemical analysis

Results of EDAX and chemical analyses are shown in Table 1. For the two Al_{13}–$AlMo_6$ compounds (obtained from both the Ho Son method and the present one), a clear coincidence is observed between experimental and theoretical values, while for the other composites, small deviations are observed (ratio Al/X/Mo = 13:2:12) according to stoichiometric values. The (%) element data are the relative weight percentage of the three elements, assuming that: %Al + %X + %Mo = 100%. The proposed formula of these Anderson heteropolyanion aluminate composites, deduced from the elemental analysis, is in agreement with that expected, i.e., $[AlO_4Al_{12}(OH)_{24}(H_2O)_{12}][XMo_6O_{24}H_6]_2 \cdot (OH) \cdot 29.5H_2O$ with X = Al(III), Cr(III), and Co(III) [1]. Similar ratios were obtained by EDAX allowing us to consider that we have no heterogeneity at the scale of EDAX analysis.

3.2. Structural properties

Figs. 1(A) and (B) show the polyhedral representation of the Keggin ε-Al_{13} isopolycation and the Anderson $[XMo_6]$ heteropolyanion, respectively, as inferred from the literature [1,11]. This Keggin isopolycation is made up of four edge-sharing triads of octahedrally coordinated aluminum atoms (Al_3O_{13}) surrounding one AlO_4 tetrahedral unit. The Anderson structure is made up of a crown of six MoO_6 octahedra surrounding one XO_6 in planar hexagonal configuration with an overall D_{3d} symmetry.

The Al_{13}–$AlMo_6$ composite exhibits a well-resolved XRD pattern similar to the one published by Ho Son et al. [1]. XRD patterns of the synthesized composites are poorly resolved and exhibit broad peaks characteristic of amorphous phase, whose position corresponds to the one observed for the aluminum reference. This allows us to consider that the amorphization is due to the Anderson anion nature.

Table 1
Chemical analysis data of prepared composites

Sample	AAS (% element)			EDAX (% element)		
	Al	Mo	X	Al	Mo	X
Al_{13}–$AlMo_6$[a]	26.0[b]	73.9[b]	–	26.0[b]	73.9[b]	–
	25.6	74.3	–	26.9	73.0	–
Al_{13}–$AlMo_6$	26.0[b]	73.9[b]	–	26.0[b]	73.9[b]	–
	25.8	73.0	–	26.5	73.4	–
Al_{13}–$CoMo_6$	21.6[b]	71.0[b]	7.2[b]	21.6[b]	71.0[b]	7.2[b]
	22.3	71.8	6.9	23.2	69.8	6.8
Al_{13}–$CrMo_6$	21.8[b]	71.6[b]	6.3[b]	21.8[b]	71.6[b]	6.7[b]
	22.5	71.6	6.5	24.3	69.1	6.4

Data are given as the relative weight percentage of different elements assuming that %Al + %Mo + %Cr = 100%.

[a] Included for comparative purposes. (Sample prepared by using the Ho Son et al. method [1].)

[b] Theoretical values.

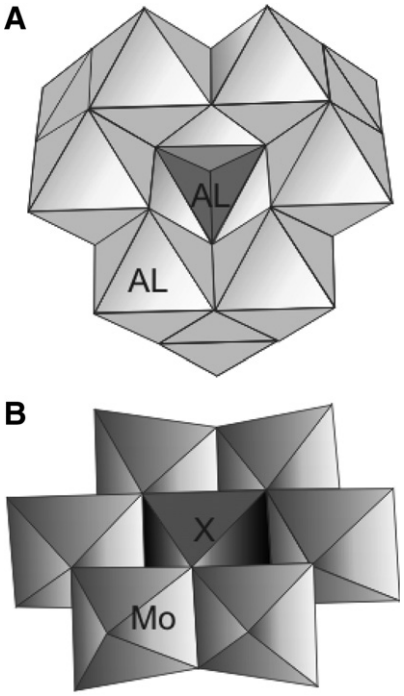

Fig. 1. Polyhedral representation of (A) ε-Al_{13} Keggin isopolycation and (B) XMo_6 Anderson heteropolyanion with X = Al, Co or Cr.

3.3. ^{27}Al nuclear magnetic resonance (NMR)

Fig. 2 shows the ^{27}Al MAS NMR spectra of Al_{13}–$AlMo_6$ and Al_{13}–$CoMo_6$. The simulation of these spectra using DMFit program [13] was performed, allowing us to obtain the isotopic chemical shift (δ_{iso}) and quad-

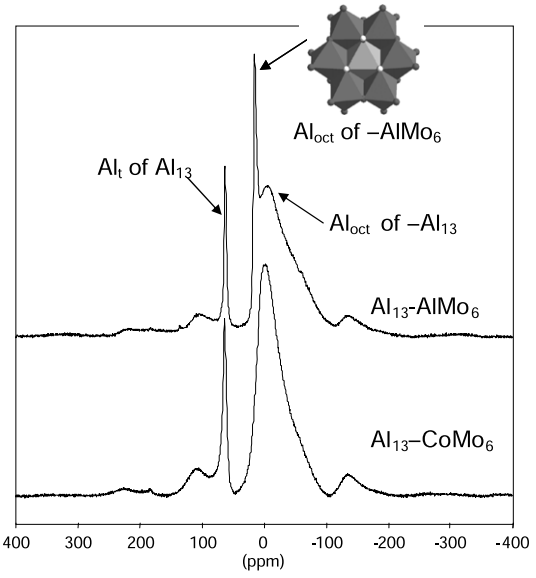

Fig. 2. ^{27}Al MAS NMR spectra of Al_{13}–XMo_6 (X = Co, Al). The polyhedral representation corresponds to the $AlMo_6$ arrangement. Ref.: Al_{oct}: Al atoms located in octahedral environment in the center of the $AlMo_6$HPA or located in octahedral environment in the Al_{13} arrangement. Al_t: Al atoms located in tetrahedral environment in the center of Al_{13} isopolycations.

rupolar parameters (C_Q and η_Q) characteristic of ^{27}Al local environments.

The spectrum of Al_{13}–$CoMo_6$ exhibits two resonances at 63 and 15 ppm assigned respectively to fourfold and sixfold coordinated aluminum atoms of Al_{13} Keggin structure. The relative intensity obtained with the fit is in good agreement with the one calculated assuming a neutral cluster (9% and 91% obtained with the simulation of the ^{27}Al MAS NMR spectra against theoretical values 7.7% and 92.3%). The line at 15 ppm is very broad due to the overlapping of six different components that could not be resolved in the experimental conditions used. Indeed, the different environment of twelve aluminum atoms was too close and differed only by a small angle deviation. On the other hand, the signal attributed to aluminum atoms located in a tetrahedral unit in the center of the Al_{13} cation was very sharp in agreement with the very symmetric environment of this atom.

These two resonance peaks are also observed in the spectrum of the Al_{13}–$AlMo_6$ composite, with however slight shifts that can be assigned to the HPA effect. In fact, for the Al_{13}–$AlMo_6$, resonances are observed at δ_{iso} equal to 61.8 and 16.3 ppm, isotopic chemical shifts that are in agreement with those reported by Allouche and coworkers for Al_{13} surrounded by sulfate anions [14], the slight shift is assigned to the nature of the counter ions. A third peak is also observed at 14.3 ppm attributed to the sixfold coordinated aluminum atoms of the $AlMo_6$ Anderson HPA [15,16]; this line is very sharp owing to the very symmetrical local environment of aluminum in this structure. The relative aluminum amounts, deduced from the fit of this ^{27}Al MAS NMR spectrum, are 13%, 79.5%, and 7.5% for the resonances located at 14.3, 16.3, and 61.8, respectively; these values are in well agreement with the theoretical values obtained considering a neutral cluster: we should obtain a relative intensity equal to 15%, 78.5%, and 6.5%.

For these two samples, the resonances assigned to the Al_{13} cation are closed. The most significant difference appears in the signal characteristic of the sixfold aluminum species that is larger for the $AlMo_6$ counter ion ($C_Q = 8.1$ MHz for Al_{13}–$CoMo_6$ and $C_Q = 9.4$ MHz Al_{13}–$AlMo_6$) suggesting that the aluminum local environment is less symmetrical in the case of Al_{13}–$AlMo_6$ than Al_{13}–$CoMo_6$. This also shows that the direct exchange of the counter ions permits the direct preparation of the $AlMo_6$ composite.

3.4. UV–vis-DR spectroscopy

Figs. 3(a) and (b) show the UV–vis-DR spectra of the Al_{13} and the ammonium salts of Anderson HPA, respectively. Whereas, the bands characteristic of the Metal ← $O^=$ charge transfer (CT) are observed at around 300 nm, the bands characteristic of "d–d" transition metal heteroatoms [Co(III) and Cr(III)] appear above 300 nm. In order to improve their analyses, the $BaSO_4$ internal standard was replaced by Al_{13}–$AlMo_6$ composite as it is shown in Fig. 4. This allows us to subtract Mo(VI) and Al(III) CT

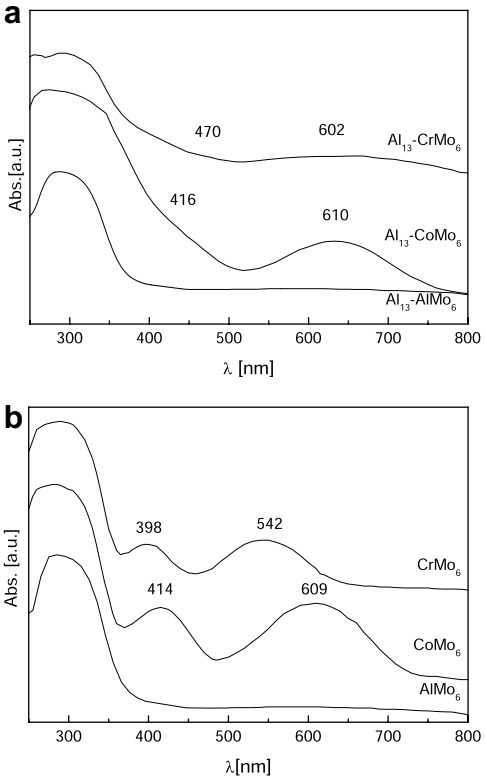

Fig. 3. UV–vis-DR spectra of (a) Al_{13}–XMo_6 composites and (b) Ammonium salts of XMo_6 heteropolyanions recorded using $BaSO_4$ as internal reference.

bands and to observe clearly Co/Cr ← $O^=$ CT and Co/Cr d–d transition bands. Thus, these spectra show CT bands of these HPA at 360 and 370 nm for the Co and Cr Anderson HPA, respectively. In the case of Co(III), the band at 610 and the shoulder at 416 nm (on the high wavelength side of Me ← $O^=$CT band) are assigned, respectively, to $^1T_{1g} \leftarrow {}^1A_{1g}$ and $^1T_{2g} \leftarrow {}^1A_{1g}$ electronic transitions, typical of Co(III) d^6 in octahedral coordination [6,17]. The d–d transition bands are broadened but are observed in the same position as those ones of the starting ammonium $CoMo_6$ Anderson salts. This confirms that the primary structure of Co(III) heteropolyanion is preserved [6,8]

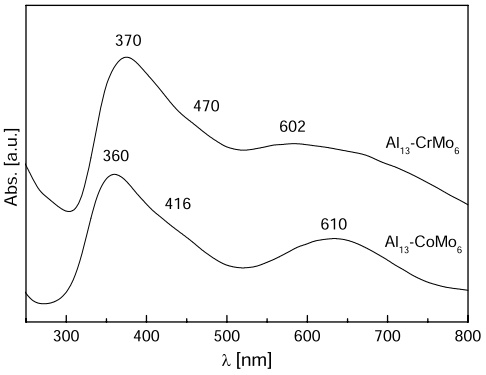

Fig. 4. UV–vis-DR spectra of Al_{13}–XMo_6 composites recorded using Al_{13}–$AlMo_6$ as internal reference.

In the case of the phase containing Cr, bands characteristic of $^4T_{2g} \leftarrow {}^4A_{2g}$ and $^4T_{1g} \leftarrow {}^4A_{2g}$ transitions are observed at 470 and 602 nm, respectively [17]. They are characteristic bands of this cation in octahedral oxygen environment [17]. This is in agreement with previous ESR studies that revealed the presence of octahedral coordinated Cr (III) in the Anderson network [10,18]. On the other hand, these studies provided direct evidence that no Al(III)–Cr(III) cation exchange occurs in the composite network whereas a dissolution of the γ-Al_2O_3 support is noticed upon impregnation with iso and heteropolyoxomolybdates and tungstate solutions suggesting the possibility of trivalent species exchange in the system [5,19].

3.5. Vibrational FT-IR and Raman spectroscopy

Fig. 5(a) shows FT-IR spectra in the 1800–400 cm^{-1} range of the three composites whereas spectra of starting Anderson phases are reported in Fig. 5(b). They are similar, even if spectra of composites exhibit broader bands. Whatever the central heteroatom (Al, Co, Cr), the main difference between the ammonium-XMo_6 and the Al_{13} composite spectra is the presence of a shoulder at 1003 cm^{-1} in spectra of composites that can be assigned to Al–OH stretching mode of Al_{13} polyoxocation [20].

The assignment of the modes of $AlMo_6$ and Al_{13}–$AlMo_6$ FT-IR and Raman spectra are given in Table 2. Regarding the assignment of different types of Mo–O bond observed in the Anderson phase, the distinction was performed according to Mo–O bonds in the D_{3d} planar structure: i.e., Mo–O_{2t} (where t stands for terminal oxygen) and Mo–Ob and Mo–Oc (standing for Mo–O–Mo and Mo–O–X bridges respectively, where X is the central heteroatom). In the lower spectral range (500–700 cm^{-1}), typical bands of XMo_6, Al_{13} and water librations are overlapped [21].

In Figs. 6(a)–(c), Raman spectra of different composites are reported, recorded below 1200 cm^{-1}. These spectra are compared to the ammonium Anderson salts. The Raman line characteristic of the MoO_{2t} symmetric stretching

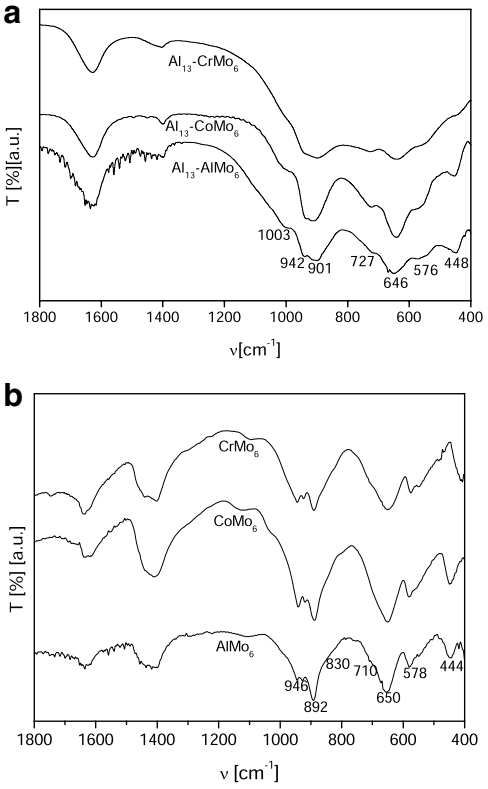

Fig. 5. FT-IR spectra of (a) Al_{13}–XMo_6 composites and (b) ammonium salts of XMo_6 heteropolyanions in the 1800–400 cm^{-1} spectral range.

modes appears at around 945 cm^{-1} in composites as a sharp and intense line, whereas the corresponding asymmetric line is weaker and noticed at lower wavenumber corresponding to those observed in IR spectroscopy (intense bands at around 892 cm^{-1} in the HPA). The shift in both types of solids, the ammonium and the composite, can be assigned to a modification of the interaction between the HPA and/or between the Al_{13} isopolycation and the corresponding HPA as previously discussed for Keggin HPA [22].

Table 2
Assignment of FT-IR and Raman spectra in the region of low energy for the $AlMo_6$ Anderson phase and for the Al_{13}–$AlMo_6$ composite, [FTIR and Raman signals in frequency (υ cm^{-1})]

$AlMo_6$		Al_{13}–$AlMo_6$		Assignment
FTIR	Raman	FTIR	Raman	
		1003 m		υ Al–OH (in [Al_{13}])
946 s	945 vs	942 s	944 vs	υs Mo–Ot
926 s				
892 vs	898 s	901 s	897 sh	υas Mo–Ot + υ Al–OH (in [$AlMo_6$])
860 sh				
830 sh				
710 sh		727 sh		υ Mo–Ob
650 vs		646 s	640 vw	
578 m	549 w	576 m	575 vw	υ Al–O
542 m				Libration H_2O
444 m	357 w	448 m	357 w	υ Mo–Oc

References: s, strong; vs, very strong; m, medium; w, weak; vw, very weak; sh, shoulder.

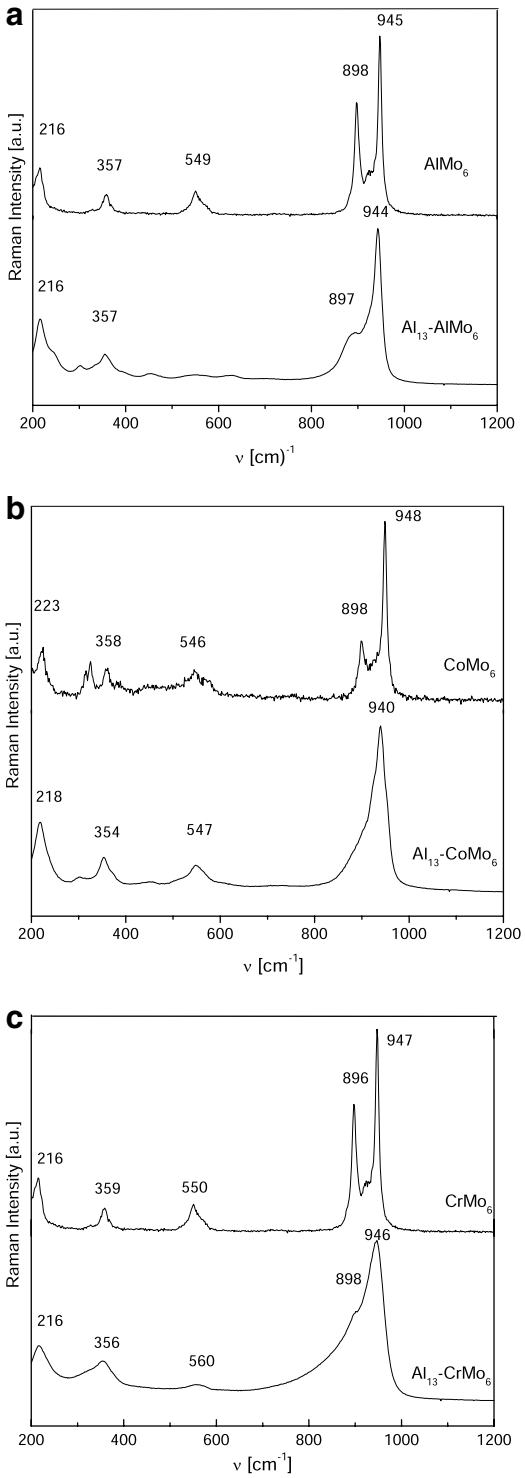

Fig. 6. Raman microprobe spectra of Al_{13}–XMo_6 and ammonium salts where X = (a) Al, (b) Co, and (c) Cr (spectral range 200–1200 cm^{-1}).

These comparisons suggest clearly that the Anderson crown structure is preserved when it is inserted in the Al_{13}-matrix, the broadening of main Raman lines is associated to the crystallinity lack as it was evidenced by XRD. So, vibrational spectroscopy (in particular Raman spectroscopy) was useful to characterize these new materials and to demonstrate that the Anderson structure in the composite lattice is preserved.

3.6. Thermal studies

Fig. 7 shows TG-DTA diagrams of studied composites. They are similar to the one reported by Ho Son et al. for the Al_{13}–$AlMo_6$ phase [1].

In the TG first steps, the weight loss up to 200 °C is around 20% which can be attributed to water departure. Fig. 8 shows Raman spectra of the Al_{13}–$CoMo_6$ composite after dehydration. The main change concerns the symmetric stretching mode of the MoO_{2t} bond that shifts from 940 to 957 cm^{-1} for Al_{13}–$CoMo_6$, from 944 to 961 cm^{-1} for Al_{13}–$AlMo_6$ and from 946 to 959 cm^{-1} for Al_{13}–$CrMo_6$ composites. These variations are assigned to the rupture of the H-bond and the subsequent reinforcement of Mo–O_{2t} bonds. The water loss (from OH groups) continued up to 600 °C (lattice collapse). Above this temperature, weak DTA exothermic signals are associated to the formation of new phases.

Fig. 9 shows comparative Al_{13}–$AlMo_6$ composite XRD patterns after different thermal treatments. The formation of aluminum molybdate ($-Al_2(MoO_4)_3$-PDF 85-2286) is clearly observed at 750 °C whereas the heating of samples up to 950 °C showed the formation of α-Al_2O_3 (PDF 75-0788). The progressive weight loss associated to the molybdate decomposition (with MoO_3 release) is observed in complementary thermal experiments above 800 °C. A similar behavior is observed for the Cr-composite where the trivalent molybdate is still observed between 800 and 950 °C. Recent ESR results of Al_{13}–$CrMo_6$ and Al_{13}–$(Cr,Al)Mo_6$ solid solution phases revealed that composite decomposition follows the Al_{13}–$CrMoO_6 \rightarrow (Cr,Al)_2(MoO_4)_3 \rightarrow (Cr,Al)_2O_3$ sequence upon heating, although the last oxide is amorphous by XRD [18].

On the contrary, the behavior of the Co-phase is different and dominated by the Co(II) ion increasing the stability by thermal treatment. Samples were XRD amorphous in the 600–750 °C temperature range due to a series of competitive processes in this studied range. In fact, the Co(III)–Co(II) reduction induced the formation of microcrystalline $CoMoO_4$ not evidenced by XRD. This hinders the $Al_2(MoO_4)_3$ formation contrary to that observed for the Al and Cr phases. The Co-system progressively transforms into $CoAl_2O_4$ spinel-phase by thermal treatment. Indeed, the UV–vis-DR spectrum of a sample heated at 800 °C exhibits the triplet at 547 (sh), 583, and 634 nm characteristic of tetrahedral Co(II) ($^4T_1(P) \rightarrow {}^4A_2$ (F) d–d transition) as well as the Mo $\leftarrow$ $O^{=}$CT band at 224 nm characteristic of the tetrahedral molybdenum environment [17,23].

The Raman spectroscopy also contributed to identify compounds formed by high temperature treatment. Fig. 10 shows Raman spectra of samples heated at 800 °C. While spectra of treated phases Al_{13}–$AlMo_6$ and Al_{13}–$CrMo_6$ exhibit lines characteristic of $Al_2(MoO_4)_3$

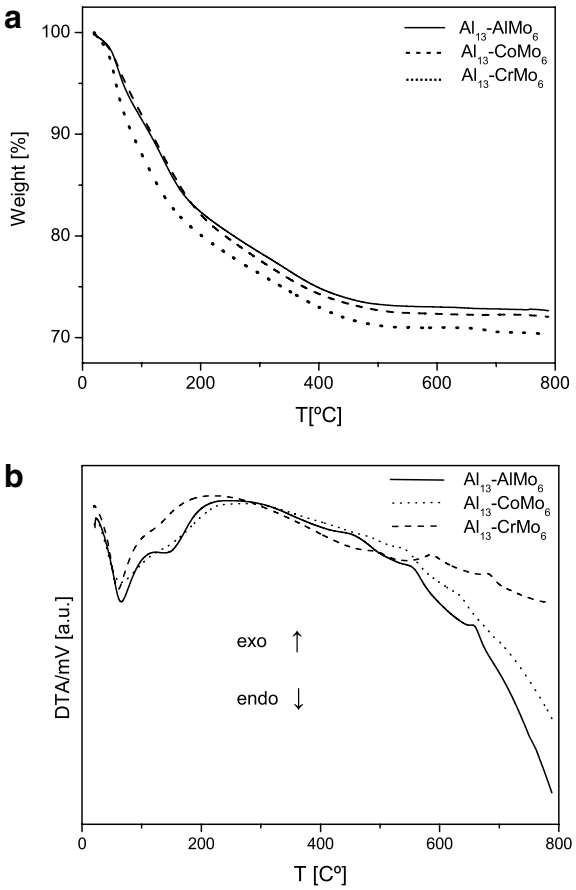

Fig. 7. (a) TG and (b) DTA diagrams of Al_{13}–XMo_6 composites.

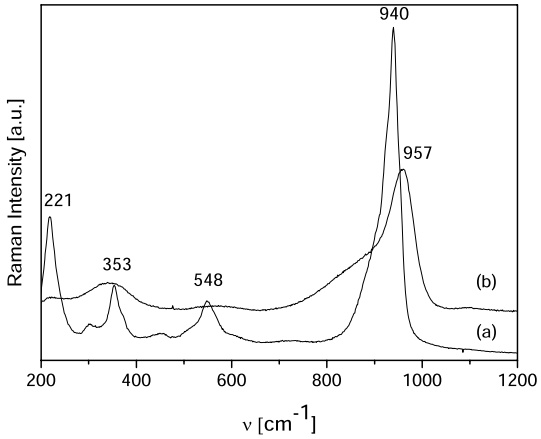

Fig. 8. Raman spectra of Al_{13}–$CoMo_6$ at (a) RT; and after heating at (b) 200 °C.

(main line at 1006 cm^{-1}), the cobalt composite spectrum exhibits also these lines but with more intense ones at 941, 952, 819 cm^{-1} corresponding to a $CoMoO_4$ crystalline phase [24].

All results allow us to formulate a decomposition scheme for Al, Co and Cr species to give the following solid phases:

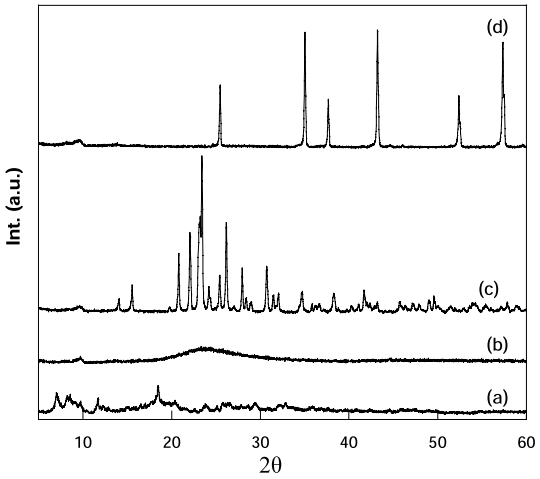

Fig. 9. XRD patterns of Al_{13}–$AlMo_6$ (a) at RT; (b) at 400 °C; (c) at 750 °C and (d) at 950 °C.

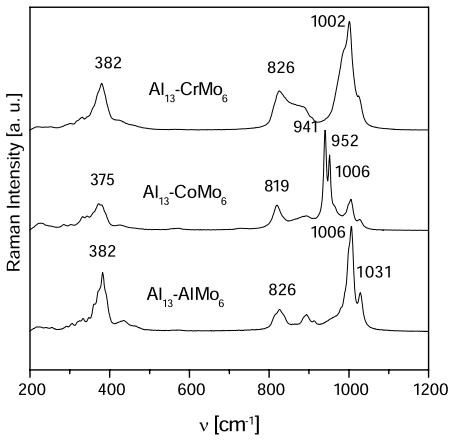

Fig. 10. Raman spectra of Al_{13}–XMo_6 composites heated at 800 °C (spectral range 200 and 1200 cm^{-1}).

$$[AlO_4Al_{12}(OH)_{24}(H_2O)_{12}][XMo_6O_{24}H_6]_2(OH)\cdot 29H_2O,$$
$$X = Al(III),\ Cr(III) \text{ and } Co(III)$$
$$\downarrow 100\text{–}200\ ^\circ C$$
$$[AlO_4Al_{12}(OH)_{24}(H_2O)_{12}][XMo_6O_{24}H_6]_2(OH)$$
$$\downarrow 200\text{–}800\ ^\circ C$$
$$X_2(MoO_4)_3,\ X = Al,\ Cr \text{ and } Co(II)(MoO_4)$$
$$\downarrow 800\text{–}950\ ^\circ C$$
$$X_2O_3,\ X = Al\text{–}Cr \text{ and } CoAl_2O_4$$

4. Conclusions

New inorganic composites interesting in the catalytic field were synthesized and characterized. They were obtained by direct combination of Al_{13} Keggin isopolycation with the Anderson heteropolyanion ($AlMo_6$, $CrMo_6$ and $CoMo_6$). This is an alternative preparation method with respect to that reported by J. Ho Son et al. that permits a direct synthesis of bulk HDS oxidic precursor

having higher textural features. The spectroscopic characterizations reveal the presence of the XMo_6 Anderson phase dispersed in a continuous matrix of Al_{13} Keggin arrangement. In addition, it is suggested that the thermal stability is related to the heteroatom nature, with the formation of X_2O_3 (X = Al, Cr) or ternary ($CoAl_2O_4$) oxides as final products.

These composites, consisting of an ordered distribution of the Anderson heteropolyanion with an Al_{13} network, would be of interest as hydrotreatment oxidic precursors. The study of their thermal stability gives us information for the direct preparation of HDS catalyst oxidic precursor. Works are now under progress to test their catalytic performance in both HDS of thiophene and ODS of dibenzothiophenes.

Acknowledgments

We are grateful to Mrs. Graciela Valle and Lic. Diego Peña for their contribution in experimental measurements. Financial support from CONICET, CICPBA (Argentina) and COFACAL Program (CNRS France and TOTAL) is gratefully acknowledged. C.I. Cabello is a member of the research staff of CICPBA, Argentina.

References

[1] J. Ho Son, H. Choi, Y.-Uk Kwon, J. Am. Chem. Soc. 122 (2000) 7432.
[2] J. Ho Son, H. Choi, Y.-Uk Kwon, O.H. Han, J. Non-Cryst. Solids 318 (2003) 186.
[3] H. Choi, Y.-Uk Kwon, O.H. Han, Chem. Mater. 11 (1999) 1641.
[4] A. Gil, L.M. Gandía, M.A. Vicente, Catal. Rev. Sci. Eng. 42 (1) (2000) 45.
[5] L. Le Bihan, P. Blanchard, M. Fournier, J. Grimblot, E. Payen, J. Chem. Soc. Faraday Trans. 94 (1998) 937.
[6] C. Martin, C. Lamonier, M. Fournier, O. Mentré, V. Harlé, D. Guillaume, E. Payen, Inorg. Chem. 43 (2004) 4636.
[7] C.I. Cabello, M. Muñoz, E. Payen, H.J. Thomas, Catal. Lett. 92 (2004) 69.
[8] C.I. Cabello, I.L. Botto, F. Cabrerizo, M.G. González, H.J. Thomas, Adsorpt. Sci. Technol. 18 (7) (2000) 591.
[9] C.I. Cabello, F.M. Cabrerizo, A. Alvarez, H.J. Thomas, J. Mol. Catal. A Chem. 186 (2002) 89.
[10] I.L. Botto, C.I. Cabello, H.J. Thomas, D. Cordischi, P. Porta, Mater. Chem. Phys. 62 (2000) 254.
[11] L. Allouche, C. Gérardine, T. Lioseau, G. Férey, F. Taulelle, Angew. Chem. Int. Ed. 39 (3) (2000) 511.
[12] A. Samoson, E. Lippma, Phys. Rev. B, Condens. Matter 28 (1983) 6567.
[13] D. Massiot, F. Fayon, M. Capron, I. King, S. Le Calvet, B. Alonso, J.-O. Durand, B. Bujoli, Z. Gan, G. Hoatson, Magn. Reson. Chem. 40 (2002) 70.
[14] L. Allouche, C. Huguenard, F. Taulelle, J. Phys. Chem. Solids 62 (2001) 1525.
[15] X. Carrier, J.-F. Lambert, M. Che, J. Am. Chem. Soc. 119 (1997) 10137.
[16] X. Carrier, J.-F. Lambert, M. Che, Stud. Surf. Sci. Catal. 130 (2000) 1049.
[17] A.B.P. Lever, in: Inorganic Electronic Spectroscopy, 2nd ed., Elsevier, Amsterdam, 1984.
[18] C.I. Cabello, I.L. Botto, J. Filace, P. Porta, G. Minelli, M. Occhiuzzi, J. Porous Mat., 13, in press.
[19] X. Carrier, J.B. D'Espinose de la Cailerie, J.F. Lambert, M. Che, J. Am. Chem. Soc. 121 (1999) 3377.
[20] I.L. Botto, A.C. Garcia, H.J. Thomas, J. Phys. Chem. Solids 53 (8) (1992) 1075.
[21] P. Diatto, M. Martini, G. Spinolo, J. Phys. Chem. Solids 49 (1988) 1139.
[22] A. Griboval, P. Blanchard, E. Payen, M. Fournier, J.L. Dubois, Stud. Surf. Sci. Catal. 106 (1997) 181.
[23] M. Fournier, C. Louis, M. Che, P. Chaquin, D. Masure, J. Catal. 119 (1989) 400.
[24] S. Sheik Saleem, G. Aruldhas, Polyhedron 1 (4) (1982) 331.